Joule-Thomson Cryogenic Nitrogen Orifice Flows

Ebony M. Bland[1], Hannah E. Cherry[2], Nicole M. Vaughn[3], Kevin W. Pedersen[4]
NASA Marshall Space Flight Center, Huntsville, Alabama, 35812, USA

Mason Lebakken[5] and
Embry-Riddle Aeronautical University Worldwide and Online,

Daytona Beach, Florida, 32114, USA

L. Catherine Potts[6]
Florida State University, Tallahassee, Florida, 32306, USA

The Joule-Thomson Effect involves the expansion of a fluid through a throttling device, often a simple orifice, resulting in a change in the fluid's temperature. It has been leveraged in the design and analysis of Thermodynamic Vent Systems and integrated into injector designs for cryogenic no-vent fill tank-to-tank transfer testing. There is a scarcity of comprehensive data available to model the phenomenon effectively using tools such as GFSSP for cryogenic nitrogen flows. This experiment aims to model the Joule-Thomson effect of liquid nitrogen through seven traditionally manufactured, sharp-edged orifices manufactured by O'Keefe and three additively manufactured (AM) orifices manufactured by Cumberland Additive. The traditional orifice sizes were 0.016, 0.02, 0.024, 0.032, 0.037, and 0.04 inch in diameter. The three additive orifices had diameters with target/nominal sizes equal to the 0.016, 0.024, and 0.04 inch O'Keefe orifices. However, the actual diameters of the AM orifices were found to be 0.014, 0.024, and 0.035 inches due to additive manufacturing restrictions. Water was flowed through the orifices to verify that their flow coefficients matched published values and to establish flow coefficients for the AM orifices. Liquid nitrogen was flowed through the orifices in a separate test apparatus. The liquid nitrogen started as a subcooled liquid upstream of the orifice and transitioned into a two-phase gas-liquid mixture after passing through each orifice. The upstream pressure was set to 29 psia, 34 psia, 39 psia, and/or 42 psia or 44 psia. The pressure, temperature, and flow rate were measured upstream and downstream of the orifice for three trials at each set point. The average volumetric flow rate and Joule-Thomson Coefficients were calculated from this data. The AM orifices and traditionally manufactured orifices displayed similar results. This data will refine the dataset GFSSP uses to model the J-T Effect more accurately.

[1] Engineer, Advanced Propulsion Research and Technology Branch
[2] Engineer, Advanced Propulsion Research and Technology Branch
[3] Engineer, Advanced Propulsion Research and Technology Branch
[4] Engineer, Advanced Propulsion Research and Technology Branch
[5] Intern, Advanced Propulsion Research and Technology Branch
[6] Intern, Advanced Propulsion Research and Technology Branch

I. Nomenclature

AM	=	Additively Manufactured
GN_2	=	Gaseous Nitrogen
C_p	=	Specific Heat Capacity at Constant Pressure
C_v	=	Flow Coefficient
JT	=	Joule-Thomson
μ_{JT}	=	Joule-Thomson Coefficient
LN_2	=	Liquid Nitrogen
$\dot{m}$	=	Mass Flow Rate
P	=	Pressure
ΔP	=	Change in Pressure
Q	=	Volumetric Flow Rate
ρ	=	Density
SG	=	Specific Gravity
T	=	Temperature
V	=	Volume
$\dot{V}$	=	Volumetric Flow Rate

II. Introduction

As NASA puts more of an emphasis on reusable cryogenic systems to enable spacecraft to venture further and further into space, it is imperative to understand not only how much fuel is necessary, but how it can be replenished. In instances where human intervention is unsafe or inaccessible, tank-to-tank transfer will need to be utilized. Cryogenic propellants (oxygen, hydrogen, methane) are commonly used for propulsion systems or are readily generated through in-situ resource utilization, making tank-to-tank transfer of these cryogenic fluids of particular importance. State-of-the-art tank-to-tank transfers use a "no-vent fill" technique so that the transfer can occur with as little propellant lost to boil off as possible while still completing the transfer as quickly as possible. However, such a transfer is difficult and relies on the ability to sub-cool the cryogenic fluid enough prior to transfer to absorb all the heat of the tank to be filled. One method of propellant cooling is the isenthalpic Joule-Thomson (JT) expansion effect. The Joule-Thomson Effect involves the expansion of a fluid through a throttling device, often a simple orifice, resulting in a change in the fluid's temperature. It has been leveraged in the design, modeling, and analysis of Thermodynamic Vent Systems (TVS) and integrated into injector designs for cryogenic no-vent fill tank-to-tank transfer testing. Therefore, understanding how cryogenic fluids behave when passing through an orifice is key to being able to establish refueling stations in orbit or in Lunar or Martian environments. The Joule-Thompson expansion effect is a relation of the rate of change of the temperature of the fluid with respect to the pressure and is defined as:

$$\mu_{JT} = \left(\frac{\partial T}{\partial P}\right)_H = \frac{V}{C_p} * (\alpha T - 1) \quad (1)$$

Where α is the coefficient of thermal expansion, C_p is the heat capacity of the fluid at constant pressure, V is the volume of the fluid, and T the temperature of the fluid. A μ_{JT} of less than 0 indicates an increase in temperature; a μ_{JT} of more than 0 indicates a decrease in temperature.

Tank-to-tank transfer tests can be difficult to thermally model, so empirical anchoring data is highly sought after. The NASA MSFC developed software tool, Generalized Fluid System Simulation Program (GFSSP), has been utilized on several occasions in the modeling of tank-to-tank cryogenic transfers. A recent project using TVS injectors was modeled with GFSSP to predict the level of subcooling that could be achieved on the injected fluid, as well as the heat transfer interactions with the tank ullage space [1]. It became apparent during that project that some additional work was needed to accurately model the JT throttling process when applied to cryogenic fluids. The series of experiments detailed in this work sought to generate a data set that could be used to update the GFSSP Joule-Thomson function when cryogenic nitrogen is used.

III. Experiment Overview

Two sets of experiments were conducted using the same set of orifices. First the water was flown through the orifices to get baseline performance values that could later be compared to LN_2 values.

A. Orifice Sizing

Ten orifices were tested with both water and LN_2. The orifice selection consisted of three additively manufactured (AM) and seven conventionally produced. The orifices are classified by diameter and are described in Table 1 below.

Table 1: Orifice types and sizes

Manufacturer	Type	Size (in)
O'Keefe	Conventional	0.016
O'Keefe	Conventional	0.020
O'Keefe	Conventional	0.024
O'Keefe	Conventional	0.028
O'Keefe	Conventional	0.032
O'Keefe	Conventional	0.037
O'Keefe	Conventional	0.040
Cumberland Additive, Inc	Additively Manufactured	0.014
Cumberland Additive, Inc	Additively Manufactured	0.024
Cumberland Additive, Inc	Additively Manufactured	0.035

B. Water Flow Test

All ten orifices were first tested with water. The schematic below illustrates the flow path of the test apparatus.

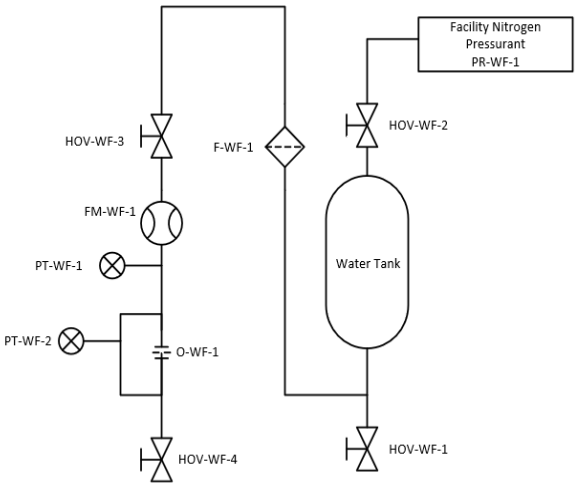

Figure 1: Water Rig Schematic

Each orifice was tested at pressures between 5 to 30 psig at increments of 5 psig. At each pressure, data from the Emerson flow meter (FM-WF-1 in Figure 1) and additional pressure sensors were recorded for one minute. In all, this resulted in six 1-minute trials, per orifice. More trials per pressure were not necessary as this experiment had already been completed earlier in 2023. The goal of repeating the experiment was more to confirm the validity and repeatability rather than to gather new data.

C. Liquid Nitrogen Flow Test

The same ten orifices tested with water were also tested with LN_2. The schematic below illustrates the flow path of the LN_2 through the test apparatus.

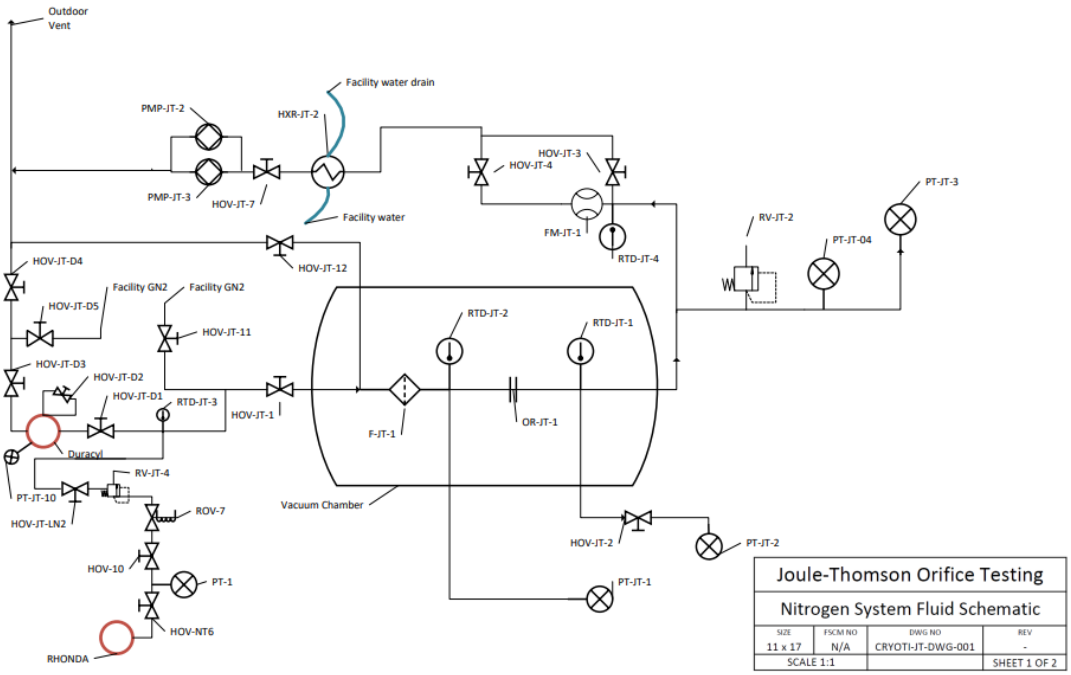

Figure 2: Nitrogen Test Rig Schematic

The overall LN2 system design was based on a similar concept to the water system. The addition of an LN_2 supply and vent system, as well as a vacuum chamber made the LN2 test configuration much more complex. The LN_2 system used facility LN_2 stored in the large outdoor Dewar (RHONDA).

In the initial design, the system included a self-pressurization system in which the LN_2 would fill up a primary vessel, and then overflow into a secondary tank with an externally controlled heat strip. This would have theoretically allowed for tighter control of the rate of boiloff and therefore the pressurization rate of the tanks. This boil-off would flow back into the larger LN_2 tank, slowly push down on the liquid, and pressurize the primary vessel. The main benefit of using this system was to regulate the boil-off rate of the liquid nitrogen, as the gaseous nitrogen (GN_2) would still be cold. Unfortunately, this system was discarded due to issues in backpressure regulation after the first few rounds of attempted testing. Facility GN_2 was used to regulate the pressure upstream of the orifice after reassessing the system design.

Once the Nitrogen passed through the orifice, the flow rate was measured using an FTI flow meter (FM-JT-1 in Figure 2). Downstream of the flow meter, the heat exchangers were used to warm the nitrogen to ensure it was fully

gaseous and could safely pass through the vacuum pumps. These pumps were included to help pull liquid nitrogen through the orifice and maintain a desirable and controllable pressure drop across the orifice.

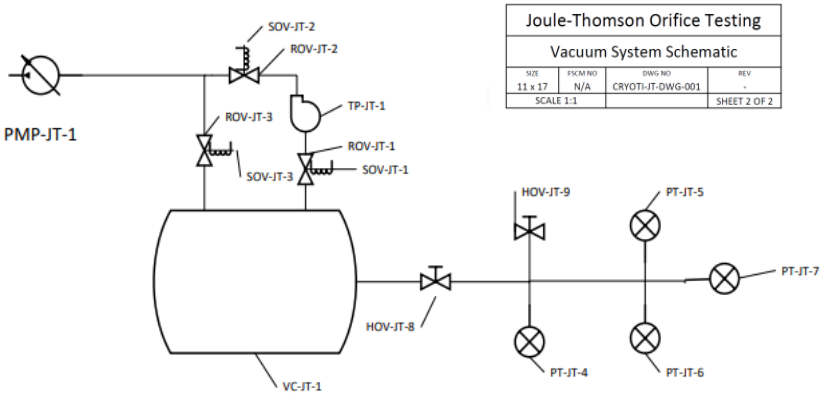

Figure 3: Vacuum System Schematic

The vacuum chamber was necessary to mitigate excess heat coming into the system and ensure saturated LN2 was entering the orifice. A roughing pump was used to get the pressure in the chamber below 1 Torr. Each orifice was targeted to test at pressures of 24, 29, and 34 psia. There were additional set point pressures due to issues reaching the desired pressure. At each set point, data was collected for temperature, flow rate, and pressure at different points in the system for 1 minute and repeated consecutively 3 times. In all, this resulted in nine 1-minute trials per orifice.

IV. Experimental Setup

A. Water Flow Rig

The water flow test rig is shown in Figure 4 below. The rig was assembled in Cell C in Lab 104 in Building 4205 at Marshall Space Flight Center.

Figure 4: Water Flow Rig Set Up

For this round of experimentation, a simple setup was used. First, a small tank, with a volume of approximately one gallon, was filled with water. Once the tank was confirmed to be full, it was connected to an air supplying pressure controller. This controller was used to pressurize the tank and thereby the system. The water was flowed through a filter, then an Emerson Coriolis flow meter to ascertain the flow rate and temperature, then through the orifice and into a catchment container. After the Emerson, a Wika pressure transducer measured the pressure upstream of the orifice, and a Tecsis differential pressure sensor measured the pressure on either side of the orifice. The dual pressure sensors were used to check each other. The data recorded consisted of volumetric flow rate (gpm), temperature (°C), pressure (psia), and differential pressure (psid).

B. Liquid Nitrogen Flow Experiment (LN2 and Vacuum)

The LN_2 experimental set up consisted of components located both inside Lab 108 and outside of building 4205 at Marshal Space Flight Center. The outside facility Dewar RHONDA was used to hold and supply the internal system with LN_2. The remaining system components were located inside of the building. The vacuum chamber housed temperature and pressure sensors both upstream and downstream of the JT orifice. A vacuum was pulled and maintained by a vacuum pump. Figure 5 shows the LN2 lines used to connect to the orifice VCR tubes.

Initially, RHONDA was to be used to supply the LN_2 for the system chill down and the execution of the experiment. Due to this process being flow restricted and therefore picking up too much heat across the flow path to the vacuum chamber, subcooled temperatures were not achieved using this approach. A secondary Dewar (Dura-Cyl) was added right a short distance from the vacuum chamber to reduce line heat pick up and ensure subcooled temperatures for the LN_2 leading into the orifice. After more unsuccessful testing attempts, a bypass leg with a larger tubing diameter was added. This bypass reduced the impact of heat gain caused by flow restriction that was preventing the fluid from achieving a subcooled status.

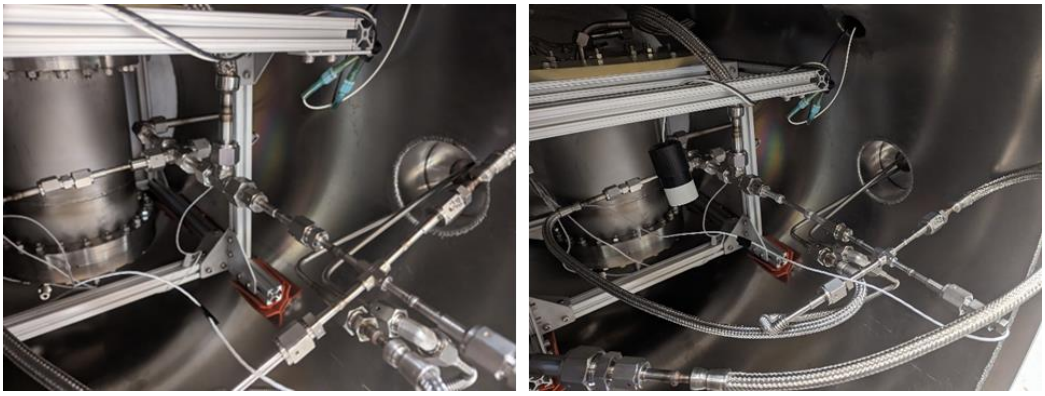

Figure 5: Orifice Set Up with Conventional (Left) and AM Orifice (Right)

The pressure across the orifice was controlled by using a combination of pressurizing the Dura-Cyl and pulling a slight vacuum on the lines downstream of the orifice with the series of vacuum pumps (varying the use between 1-3 pumps, depending on the size of the orifice). The system had to be adequately chilled before opening the leg that housed the flow meter to prevent over spinning the turbine. The cold fluid was passed through a heat exchanger to reduce the temperature enough to avoid damage that would be caused by passing LN2 through the vacuum pumps. Data collection was initiated once the measured temperature upstream of the orifice reached subcooled status.

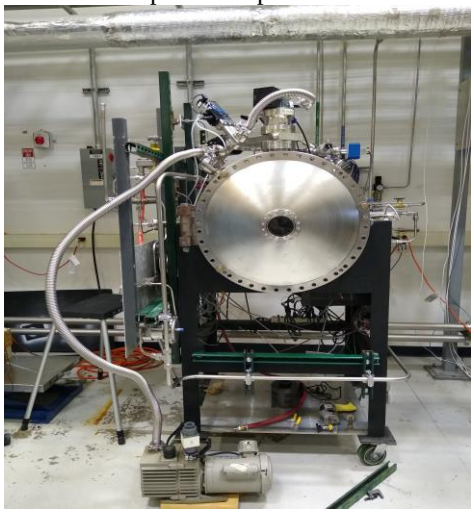

Figure 6: Vacuum Chamber and Roughing Pump

V. Experimental Procedure

For both the water and LN_2 testing, LabView software was used to record all sensor information for 1 minute for each trial, with a sampling rate of 1 Hz.

A. Water Flow Rig

The water flow testing was performed in Cell C in Lab 104 in Building 4205 at MSFC. The small holding tank was filled with water that was supplied from facility water. Once the tank was confirmed to be full, the supply line was disconnected, and the tank was connected to a pressure regulator that was driven by facility supplied air. Once the initial test pressure of 5psi was reached on the pressure regulator, the valve downstream of the tank was opened, and the water was allowed to flow through the system. When the temperature and pressure being measured by the system stabilized, recording began, and the test ran for 1 minute. After the initial run, the pressure was increased in increments of 5 psig up to 30 psig, for a total of 6 tests per orifice.

B. Nitrogen Flow Rig

The LN_2 flow testing was performed in a small vacuum chamber in Lab 108 in Building 4205 at MSFC. Once the orifice was installed, the vacuum chamber would be sealed and pumped down to below 1 Torr. The Nitrogen system would then be purged using facility GN_2 to ensure no other fluids were present in the lines. The bulk storage tank (RHONDA) of LN_2 would be pressurized and supply LN_2 to fill the Dura-Cyl tank, positioned right next to the vacuum chamber. Once the Dura-Cyl was full, the RHONDA supplied LN_2 would then be directed through the system to properly chill the lines in preparation for the test. The downstream vacuum pumps and the heat exchangers would be turned on at this time. Once the system was adequately chilled, the LN_2 supply from RHONDA was turned off, and the Dura-Cyl was pressurized with facility GN_2. When the pressure in Dura-Cyl reached desired test pressure, the LN_2 from Dura-Cyl was flowed through the system and data recording was begun. After the minute had elapsed, the pressure in Dura-Cyl was increased to each of the desired test pressures and the process repeated until the test was complete, or the LN_2 ran out, whichever came first. This process was repeated for each of the orifices.

VI. Data Analysis and Results

A. Water Testing

In the water flow test, the flow rates through each traditionally manufactured orifice and AM orifice were recorded at different tank pressures. The flow rate data for the traditional orifices was compared to published flow rate data provided by the manufacturer, O'Keefe. Figure 8 compares the measured flow rate values to the published values for the O'Keefe orifices. Measured values are shown as solid lines, while the manufacturer's published data is displayed as dotted lines of the same color.

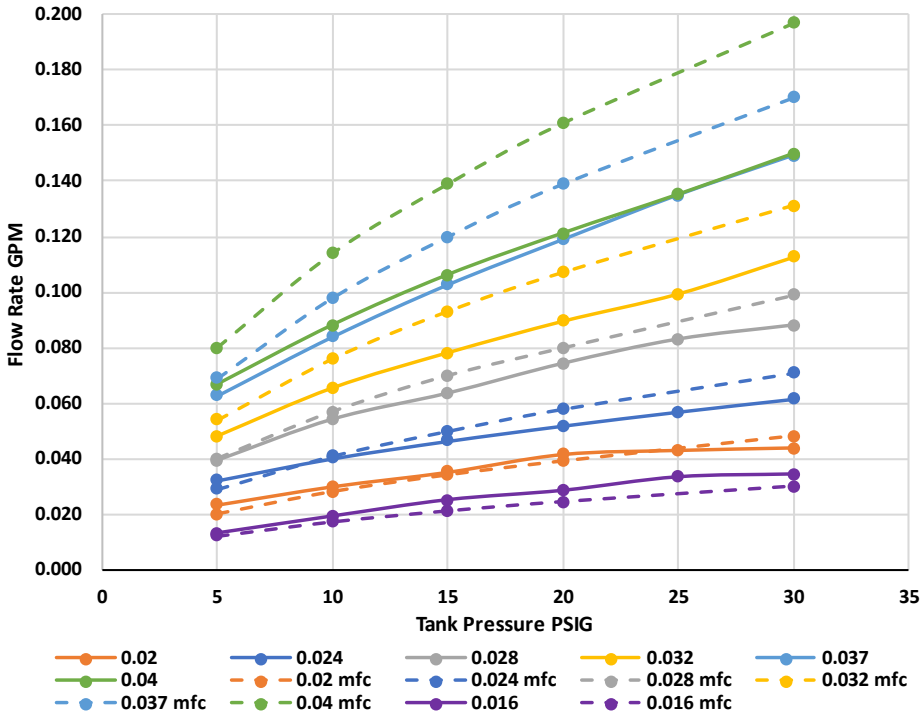

Figure 7: Comparison of Measured and Published Flow Rates for O'Keefe Orifices.

The empirical relationship between flow rate and pressure changes for the O'Keefe orifices aligns closely with published data. On average, there is a difference of 10% to 25% between the published and measured flow rate trends, with larger discrepancies observed in the flow rate measurements of the larger orifices. Additionally, the flow rates of the additively manufactured orifices were measured at various tank pressures, although these results are not presented

in Figure 9. Equation 2 was used to calculate the average flow coefficients for all the orifices, which were then compared to the published data. The flow coefficient, C_v, was calculated using flow rate Q, specific gravity of water SG, and pressure differential across each orifice, ΔP.

$$C_v = Q\sqrt{\frac{SG}{\Delta P}} \qquad (2)$$

Table 2 summarizes the measured flow coefficients of both conventional and AM orifices, comparing them to the published values from O'Keefe Controls Co [2]. Cumberland Additive did not provide published flow coefficient data for the AM orifices. The AM orifices are compared to equally sized O'Keefe-manufactured orifices. For example, the 0.014-inch AM orifice is compared to a 0.014-inch O'Keefe orifice.

Table 2: Flow Coeffcients

Orifice Size	Average Measured	Published Values	% Difference
0.014 AM (0.016 Nom.)	0.0030	0.0043	30%
0.016	0.0056	0.0055	1%
0.02	0.0092	0.0090	2%
0.024	0.0130	0.0130	0%
0.024 AM (0.028 Nom).	0.0153	0.0130	17%
0.028	0.0187	0.0180	4%
0.032	0.0234	0.0240	3%
0.037	0.0316	0.0310	2%
0.04	0.0325	0.0360	10%
0.035 AM (0.04 Nom.)	0.0355	0.0280	27%

The results show that all the conventionally manufactured orifices measured within 10% of the published values from the manufacturer. However, the AM orifices exhibited a wider variation, averaging about a 30% percent difference. This discrepancy likely results from surface roughness affecting the measurable internal diameter of the printed orifices. The water flow test established flow coefficients for the AM orifices and validated the performance of the conventional orifices within an acceptable range. Overall, the results indicate that this procedure is suitable for proceeding to the Liquid Nitrogen Joule Thompson Testing using a similar approach.

B. Liquid Nitrogen Testing

Figure 10 illustrates the saturation curve for liquid nitrogen from data obtained from NIST[4]. Pressure and temperature data for upstream and downstream conditions at each orifice are also displayed in Fig 10. All upstream data points are represented as X's, while downstream points are represented as O's. Each color corresponds to a different orifice, as referenced in the legend.

During the liquid nitrogen testing, the liquid was maintained at pressures of 29 psia, 34 psia, and between 39 psia and 42 psia, with temperatures ranging from 80 K to 82 K upstream of each orifice. One outlier trial was conducted at 44 psia and 84 psia during testing with the 0.04 inch orifice. As shown in Figure 10, these conditions place the fluid in the subcooled liquid region initally. The objective was to pressurize the liquid nitrogen to control intial state and achieve subcooling. Subcooled initial conditions are ideal for modeling cryogenic applications because cryogenic propellants are stored as subcooled liquids [3].

[4] NIST Office of Data and Informatics, Nitrogen Available: https://webbook.nist.gov/cgi/cbook.cgi?ID=C7727379&Mask=4.

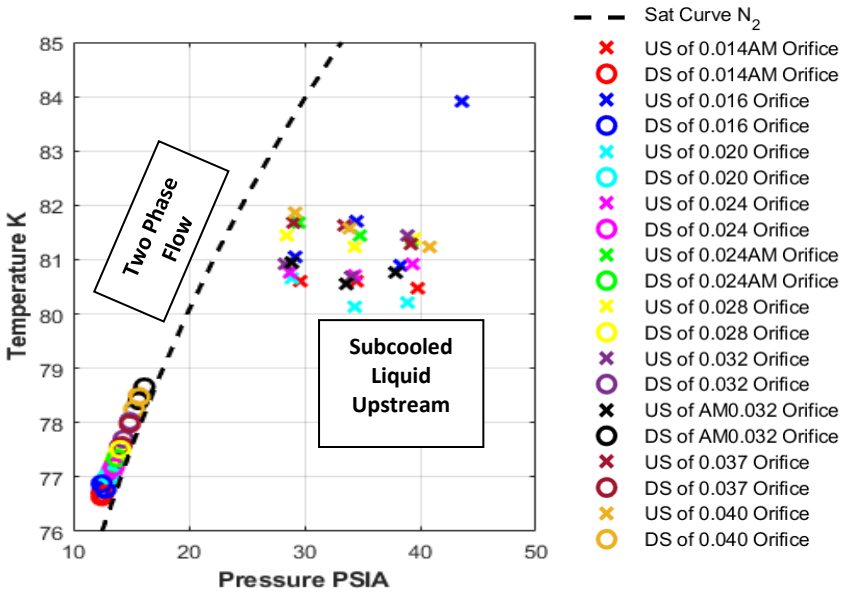

Figure 8: Pressure and Temperature Data on Nitrogen Phase Diagram

As the subcooled liquid nitrogen flows through the orifice, it experiences Joule-Thomson expansion, leading to a phase change and a decrease in both pressure and temperature. In Figure 10, the downstream pressure falls to between 12 psia and 18 psia, with temperatures ranging from 76 K to 79 K. Based on the graph, the fluid is positioned just above the saturation line, indicating that it is in a two-phase flow state. This phase change was an expected behvior for each orifice and desireble due to the cooling effects. This phase change is an expected behavior for each orifice and is desirable due to the cooling effects. Although the temperature decrease is between 2 - 5 K, the combination of multiple orifices would lead to a greater temperature reduction when implemented in a Thermal Vent System to cool a propellant tank. The Joule-Thomson expansion that liquid nitrogen undergoes can be mathematically represented by the Joule-Thomson Coefficient. This coefficient describes the rate of change of the temperature of the fluid with respect to pressure and is defined in Eqn (1).

For each test run at different upstream pressures with each orifice, the Joule-Thomson Coefficient was calculated. The variation of observable factors was investigated to examine their relationship with the Joule-Thomson Coefficient. This included orifice sizes, the performance of traditional versus additively manufactured orifices, exhaust flow rate, and how pressure and temperature change during the Joule-Thomson process.

Table 3 summarizes the Joule-Thomson coefficient (K/Psia) for each orifice at various upstream pressures. Some cells contain “N/A” because only the 0.016 inch and 0.04 inch orifices were tested at additional upstream pressure settings of 42 psia and 44 psia respectively. This additional test trial was due to pressure overshoot and issues with maintaining subcooled liquid phase with nitrogen upstream of orifice. Figure 10 graphically displays this data except for the 44psia setpoint data for the 0.016 inch orifice. AM orifice are shown with diamond markers and dashed lines and conventional orifices are shown with circle markers and solid lines. Each color represents a different upstream pressure.

Table 3: JT Coefficient Summary

Orifice Size inch	29 psia	34 psia	39 psia	42 psia	44 psia
0.014 AM (0.016 Nom.)	0.23	0.18	0.14	N/A	N/A
0.016	0.26	0.22	0.16	N/A	0.23
0.02	0.23	0.15	0.12	N/A	N/A
0.024	0.24	0.17	0.15	N/A	N/A
0.024 AM (0.028 Nom.)	0.28	0.20	0.16	N/A	N/A
0.028	0.28	0.19	0.15	N/A	N/A
0.032	0.24	0.15	0.14	N/A	N/A
0.035 AM (0.04 Nom.)	0.20	0.12	0.10	N/A	N/A
0.037	0.29	0.21	0.14	N/A	N/A
0.04	0.25	0.21	N/A	0.11	N/A

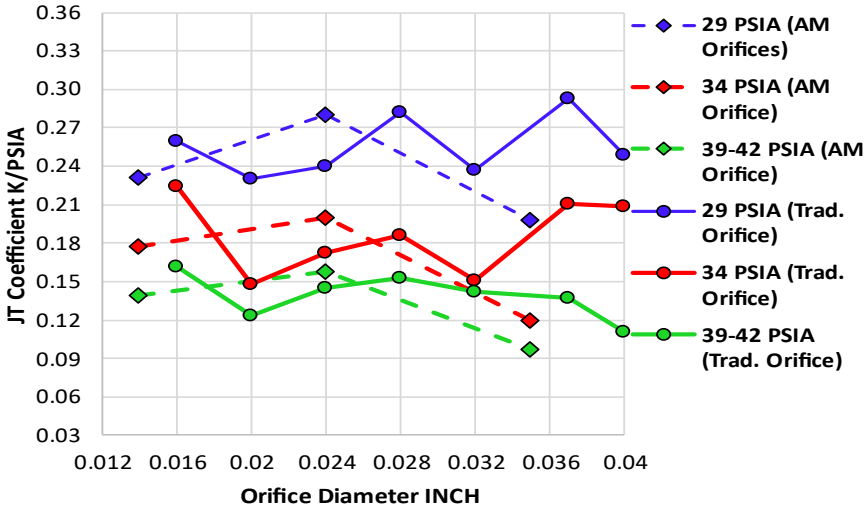

Figure 9: Joule Thomson Coefficient vs. Orifice Size

Both Table 3 and Figure 9 indicate that there is not a significant change in the Joule-Thomson coefficient with respect to increasing orifice diameter for conventional and AM orifices. For instance, at an upstream pressure of 29 psia, the variance in Joule-Thomson coefficient data with respect to orifice size is one magnitude less than the variance with respect to upstream pressure. This is consistent with the understanding that the Joule-Thomson coefficient is dependent on fluid properties rather than on restriction diameter. Additionally, Figure 9 shows no evident relationship between the Joule-Thomson coefficient and orifice diameter for both types of orifices. Instead, there is a more pronounced change in the Joule-Thomson coefficient as upstream pressure increases, with the coefficient decreasing as the upstream pressure rises. This correlation is a result of the definition of the JT coefficient, shown in Eqn.1. In summary, Figure 9 and Table 3 show that as pressure increases upstream of the orifice, there is a smaller cooling effect.

Although orifice size does not directly impact the JT coefficient it does indirectly influence the pressure drop and flowrate of the fluid undergoing a Joule Thomson expansion. Figure 10 graphically depicts the pressure drop experienced across each orifice for each setpoint. As shown in Figure 10, the pressure differential grows smaller as

the orifice size/diameter increases. This decrease is approximately 1-3 psia for the traditional orifices from smallest orifice to largest and 4-5 psia for the AM orifices. This relationship causes the denominator in the in Eqn (1) to get smaller and increase the overall JT coefficient value as the orifice size increases.

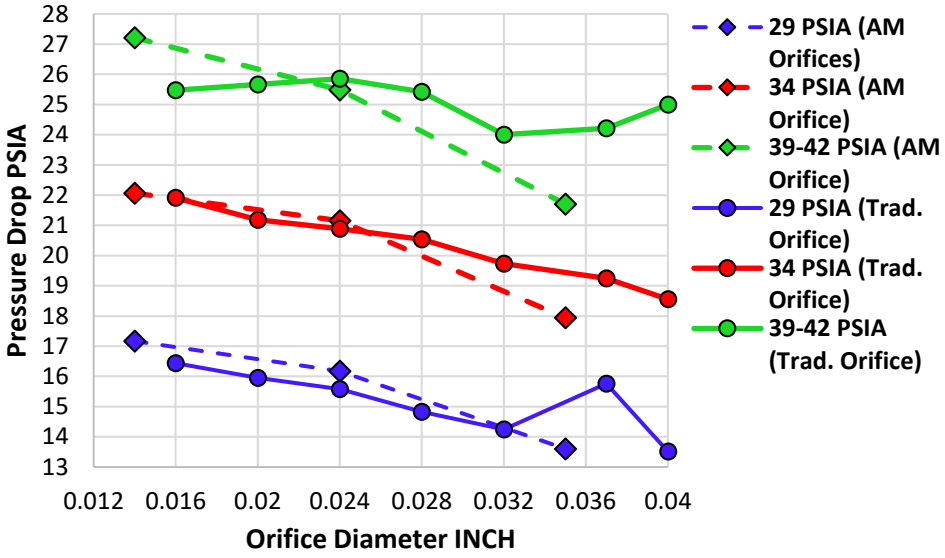

Figure 10: Pressure Drop with Respect to Orifice Size

In the Liquid Nitrogen Test, flow rate was measured downstream of the orifice when the flow was expected to be primarily gas. Table 4 lists the average flow rate through each orifice at varying upstream pressures, presented in cubic feet per second (ft^3/s). The flow rate remained constant across changes in upstream pressure, although some discrepancies occurred in certain orifices due to nitrogen pooling and the freezing of the flow meter during testing.

Table 4: Exhaust Flowrate (Cubic Feet Per Second) with Upstream Pressure

Orifice Size inch	29 psia	34 psia	39 psia	42 psia	44 psia
0.014 AM (0.016 Nom.)	0.20	0.20	0.19	N/A	N/A
0.016	0.21	0.58	0.24	N/A	0.87
0.02	0.98	0.96	0.98	N/A	N/A
0.024	0.85	0.61	0.56	N/A	N/A
0.024 AM (0.028 Nom.)	1.03	0.65	0.72	N/A	N/A
0.028	0.90	0.57	0.53	N/A	N/A
0.032	0.67	0.49	0.57	N/A	N/A
0.035 AM (0.04 Nom.)	0.68	0.49	0.47	N/A	N/A
0.037	0.76	0.63	0.74	N/A	N/A
0.04	0.55	0.70	N/A	0.66	N/A

A turbine flow meter, FM-JT-1, was used to measure the flowrate. The turbine flow meter used in this experiment is restricted to gas only with densities above 0.04 lbm/ft^3 to provide a valid reading. The density was validated through calculations, with averages shown in Table 4 and reported in pounds per cubic foot. Density calculations relied on pressure and temperature data from PT-JT-2 and RTD-JT-1, situated downstream of the orifice and upstream of the flow meter. These measurements were input into the following equation to calculate density:

$$\rho = \frac{PM}{RT} \qquad (3)$$

Where ρ is density, P is pressure, M is molar mass, R is universal gas constant, and T is temperature of the fluid. The time average density was calculated for the duration of each trial corresponding to the upstream pressure and orifice size.

Table 5: Density (Pounds Per Cubic Feet) Calculated Near Flowmeter

Orifice Size inch	29 psia	34 psia	39 psia	42 psia	44 psia
0.014 AM (0.016 Nom.)	0.09	0.09	0.10	N/A	N/A
0.016	0.10	0.11	0.09	N/A	0.13
0.02	0.10	0.11	0.13	N/A	N/A
0.024	0.16	0.17	0.18	N/A	N/A
0.024 AM (0.028 Nom.)	0.14	0.16	0.17	N/A	N/A
0.028	0.14	0.15	0.15	N/A	N/A
0.032	0.18	0.20	0.19	N/A	N/A
0.035 AM (0.04 Nom.)	0.20	0.22	0.24	N/A	N/A
0.037	0.15	0.16	0.17	N/A	N/A
0.04	0.17	0.20	N/A	0.19	N/A

Due to the turbine mechanism, the flow meter used required that the fluid flowing through it be mostly gas with a minimum density of 0.04 lbm/ft^3 to not overspin the turbine and break the flow meter. The density values in Table 5 confirm that this test series maintained the minimum density requirement, allowing the flow meter readings to be considered valid based on density criteria. Additionally, the density of liquid nitrogen is approximately 50.46 lbm/ft^3, significantly above any calculated densities downstream of the orifice, further confirming that the fluid flowing through the flow meter was not predominantly liquid.

The performance between the AM and O'Keefe orifices was evaluated by comparing the temperature reduction across each orifice in relative to upstream pressure. Figure 11 illustrates the average temperature drop at each upstream setpoint pressure for both traditional and AM orifices with comparable nominal diameters.

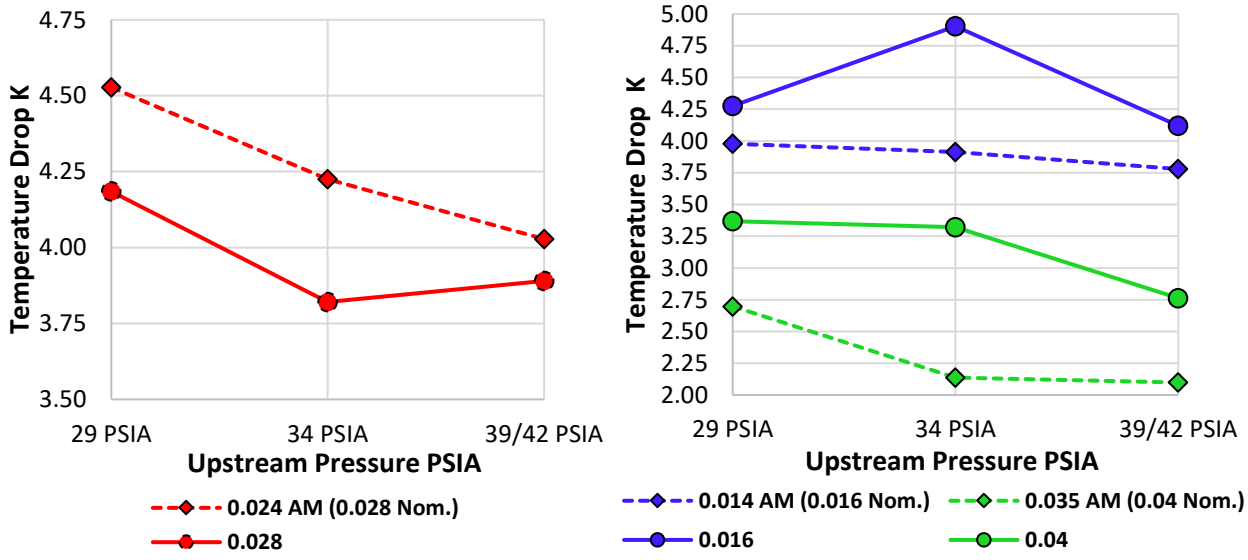

Figure 11: Comparison of Temperature Drop Between AM and Conventional Orifices

Most orifices exhibited a slightly smaller temperature drop as the upstream pressure increased and the pressure differential expanded. The maximum reduction in temperature drop was less than 2 Kelvin for each orifice as the upstream increased. Notably, the difference in temperature drop between the AM and traditional orifices was less than 2 Kelvin. This finding is surprising, given the inconsistencies associated with the printing and sizing of AM orifices. Moreover, the AM orifices and their corresponding nominal-sized conventional orifices have similar JT values, varying by only 0.01 K/psia to 0.08 K/psia, as illustrated in Figure 9. Both types of orifices also exhibit a similar decrease in JT values with increasing setpoint pressure. Additionally, their pressure drops were comparable, differing by no more than 3 psia at each setpoint.

VII. Conclusions

This data demonstrates that these orifices produce a Joule-Thomson cooling effect on subcooled liquid nitrogen, resulting in a reduction in temperature and pressure. While the Joule-Thomson coefficient is not directly affected by orifice size, it is indirectly influenced through the pressure drop associated with orifice size. Additionally, the test showed that additively manufactured orifices can be printed slightly smaller than their nominal design diameter. However, they perform comparably to their corresponding nominal sized conventional manufactured orifices, with negligible loss in performance regarding temperature reduction and pressure drop. This information is useful because it demonstrates that AM orifices are viable options and would work in additively manufactured Thermal Vent Systems used to cool cryogenic propellant tanks. Thus, providing a low-cost option and more design freedom for TVS injectors.

This research also provided valuable data to fill existing knowledge gaps concerning the Joule-Thomson effect on cryogenic flow, particularly for nitrogen, as there are limited resources available for the JT effect on nitrogen. In addition, a test rig was developed that can be used for further modeling of the Joule-Thomson effect with nitrogen using various orifices and other JT devices. This test apparatus could be adapted and used with other cryogenic fluids as well. However, some challenges arose during the testing of the smaller orifices due to low flow rates, which caused the fluid to pool and consequently warm. The complexities associated with small and cold components were significant. Measuring flow rates proved difficult because of the restrictions posed by turbine flow meters. Therefore, employing an alternative flow measurement device will be necessary for future experiments with the test rig.

Acknowledgments

The authors wish to acknowledge the use of Grammarly AI-assisted writing software features while preparing this paper[5]. The software was prompted to provide suggestions for spell-checking, grammar correction, and improving the readability of this paper. The tool was solely used for linguistic improvement and clarity.

References

[1] Vaughn, N., Belcher, T., Hines, C., Mireles, O., Pedersen, K., Smith, J., Stephens, J. and Rhys, N., "Testing of TVS Augmented Injectors for Tank-to-Tank Transfers of Cryogens," *AIAA SciTech 2023 Forum*, AIAA, National Harbor, MD & Online, 2023. doi: 10.2514/6.2023-2360

[2] O'Keefe Controls, "Precision Orifice Catalog," 4/1/10 Rev.7, pp. 23.

[3] Mustafi, S., Johnson, W., Kashani, A., Jurns, J., Kutter, B., Kirk, D., and Shull, J., "Subcooling for Long Duration In-Space Cryogenic Propellant Storage," *AIAA SPACE 2010 Conference and Exposition*, AIAA, AIAA Paper 2010-8869, Anaheim, CA, 2010.

[4] Stephen, S., "Acquisition and Correlation of Cryogenic Nitrogen Mass Flow Data Through a Multiple Orifice Joule-Thomson Device," NASA TM-103121, 1990.

[5] Jurns, J., "Visco Jet Joule-Thomson Device Characterization Tests in Liquid Methane," NASA CR- 2009-215497, 2009.

[6] Roul, M., Jena, J., and Dash, S., "Mathematical Modeling of Two-phase Flow Through Thin Orifices in Horizontal Pipes," *Proceedings of International Conference on Theoretical, Applied, Computational and Experimental Mechanics*, International Conference on Theoretical, Applied, Computational and Experimental Mechanics, ICTACEM-2010/265, IIT Kharagpur, India, 2010.

[5] https://app.grammarly.com/